9-2022

Tetrahydrocurcumin Improves Lipopolysaccharide-induced Myocardial Dysfunction By Inhibiting Oxidative Stress and Inflammation Via JNK/ERK Signaling Pathway Regulation

Hanzhao Zhu

Liyun Zhang

Hao Jia
Sacred Heart University, jiah@mail.sacredheart.edu

Lu Xu

Yu Cao

See next page for additional authors

Recommended Citation

Zhu, H., Zhang, L., Jia, H., Xu, L., Cao, Y., Zhai, M., Li, K., Xia, L., Jiang, L., Li, X., Zhou, Y., Liu, J., Yu, S., & Duan, W. (2022). Tetrahydrocurcumin improves lipopolysaccharide-induced myocardial dysfunction by inhibiting oxidative stress and inflammation via JNK/ERK signaling pathway regulation. *Phytomedicine : International Journal of Phytotherapy and Phytopharmacology*, *104*(154283), 154283.Doi.org/10.1016/j.phymed.2022.154283

Phytomedicine 104 (2022) 154283

Contents lists available at ScienceDirect

Phytomedicine

journal homepage: www.elsevier.com/locate/phymed

Original Article

Tetrahydrocurcumin improves lipopolysaccharide-induced myocardial dysfunction by inhibiting oxidative stress and inflammation via JNK/ERK signaling pathway regulation

Hanzhao Zhu [a,1], Liyun Zhang [a,1], Hao Jia [b,1], Lu Xu [c], Yu Cao [c], Mengen Zhai [a], Kaifeng Li [d], Lin Xia [e], Liqing Jiang [a], Xiang Li [a], Yenong Zhou [a], Jincheng Liu [a], Shiqiang Yu [a,*], Weixun Duan [a,*]

[a] Department of Cardiovascular Surgery, The First Affiliated Hospital, The Air Force Medical University, Xi'an, Shaanxi 710032, China
[b] Department of Chemistry, Sacred Heart University, Fairfield, CT 06825, United States
[c] Department of Chinese Materia Medica and Natural Medicines, School of Pharmacy, The Air Force Medical University, Xi'an, Shaanxi 710032, China
[d] Basic Medical Teaching Experiment Center, Basic Medical College, The Air Force Medical University Xi'an, Shaanxi 710032, China
[e] Department of Cardiovascular Surgery, General Hospital of Northern Theater Command, Shenyang, Liaoning 110015, China

ARTICLE INFO

Keywords:
Tetrahydrocurcumin
Septic cardiomyopathy
Inflammation
Oxidative stress

ABSTRACT

Background: Acute myocardial dysfunction in patients with sepsis is attributed to oxidative stress, inflammation, and cardiomyocyte loss; however, specific drugs for its prevention are still lacking. Tetrahydrocurcumin (THC) has been proven to contribute to the prevention of various cardiovascular diseases by decreasing oxidative stress and inflammation. This study was performed to investigate the functions and mechanism of action of THC in septic cardiomyopathy.

Methods: After the oral administration of THC (120 mg/kg) for 5 consecutive days, a mouse model of sepsis was established via intraperitoneal lipopolysaccharide (LPS, 10 mg/kg) injection. Following this, cardiac function was assessed, pathological section staining was performed, and inflammatory markers were detected.

Results: Myocardial systolic function was severely compromised in parallel with the accumulation of reactive oxygen species and enhanced cardiomyocyte apoptosis in mice with sepsis. These adverse changes were markedly reversed in response to THC treatment in septic mice as well as in LPS-treated H9c2 cells. Mechanistically, THC inhibited the release of pro-inflammatory cytokines, including tumor necrosis factor alpha, interleukin (IL)-1β, and IL-6, by upregulating mitogen-activated protein kinase phosphatase 1, to block the phosphorylation of c-Jun N-terminal kinase (JNK) and extracellular signal-regulated protein kinase (ERK). Additionally, THC enhanced the levels of antioxidant proteins, including nuclear factor-erythroid 2-related factor 2, superoxide dismutase 2, and NAD(P)H quinone oxidoreductase 1, while decreasing $gp91^{phox}$ expression. Furthermore, upon THC treatment, Bcl-2 expression was significantly increased, along with a decline in Bax and cleaved caspase-3 expression, which reduced cardiomyocyte loss.

Conclusion: Our findings indicate that THC exhibited protective potential against septic cardiomyopathy by reducing oxidative stress and inflammation through the regulation of JNK/ERK signaling. The findings of this study provide a basis for the further evaluation of THC as a therapeutic agent against septic cardiomyopathy.

Abbreviations: CCK-8, cell counting kit-8; CK-MB, creatine kinase isoenzyme MB; cTnI, cardiac troponin I; ERK, extracellular signal-regulated protein kinase; HE, hematoxylin and eosin; IL, interleukin; JNK, c-Jun N-terminal kinase; LDH, lactate dehydrogenase; LPS, lipopolysaccharide; LVEF, left ventricular ejection fraction; LVFS, left ventricular fractional shortening; MAPKs, mitogen-activated protein kinases; NQO1, NAD(P)H quinone oxidoreductase 1; Nrf2, nuclear factor-erythroid 2-related factor 2; ROS, reactive oxygen species; SOD2, superoxide dismutase 2; THC, tetrahydrocurcumin; TUNEL, terminal deoxynucleotidyl transferase dUTP nick-end labeling.

* Corresponding authors.
E-mail addresses: yushiq@fmmu.edu.cn (S. Yu), duanweixun@126.com (W. Duan).
[1] These authors contributed equally to this work.

https://doi.org/10.1016/j.phymed.2022.154283
Received 24 March 2021; Received in revised form 6 June 2022; Accepted 17 June 2022
Available online 18 June 2022

Introduction

Sepsis is a systemic inflammatory response syndrome that develops in patients in response to severe infection, causing approximately five million deaths globally each year (Fleischmann et al., 2016). As a result of the aberrant systemic inflammatory reaction, multiple organs, including the heart, kidney, liver, and brain, may become dysfunctional and injured (Caraballo and Jaimes, 2019; Parrillo et al., 1990). Septic cardiomyopathy, the most serious and difficult-to-treat complication, reportedly occurs in approximately 50% of patients with sepsis, with a mortality rate of 70% to 90% (Vieillard Baron et al., 2008). However, to date, no clinically effective drug has been developed for the treatment of septic cardiomyopathy.

Numerous mechanisms, including mitochondrial injury, oxidative stress, metabolic imbalance, and inflammation, have been reported to contribute to the pathological process of septic myocardial dysfunction (Flynn et al., 2010; Lv and Wang, 2016). Among these, inflammation and oxidative damage are considered the major factors underlying the onset and progression of septic cardiomyopathy (Suzuki et al., 2017; Mantzarlis et al., 2017). During sepsis, as a result of the excessive release of pro-inflammatory cytokines, such as tumor necrosis factor alpha (TNF-α) and interleukins (ILs), in the serum, a large number of immune cells are activated within the myocardium, stimulating reactive oxygen species (ROS) generation, which in turn contributes to cardiomyocyte apoptosis (Sato et al., 2002). Inflammatory infiltrates exacerbate cardiomyocyte loss and myocardial dysfunction, potentially leading to heart failure. Therefore, inhibition of the inflammatory response and ROS generation is of major importance in the treatment of septic cardiomyopathy.

Tetrahydrocurcumin (THC), a hydrogenation product of curcumin, is isolated from the rhizome of turmeric and exhibits various biological properties, especially anti-oxidative and anti-inflammatory properties (Park et al., 2016; Chen et al., 2018). The ability of THC to attenuate oxidative damage is attributed to its activity as a free radical scavenger (Luo et al., 2019; Vacek et al., 2018). Furthermore, emerging evidence suggests that THC treatment mitigates the inflammatory response by blocking the nuclear factor kappa B signaling pathway (Zhang et al., 2018; Pan et al., 2020). c-Jun N-terminal kinase (JNK) and extracellular signal-regulated protein kinase (ERK), as mitogen-activated protein kinases (MAPKs), are effector molecules involved in initiating inflammation and oxidative stress and are thus targeted by various clinical drugs (Xie et al., 2014; Huang et al., 2018; Song et al., 2020). Notably, the regulation of the MAPK pathway is reliant on mitogen-activated protein kinase phosphatase-1 (MKP-1), which is a major phosphatase that specifically dephosphorylates JNK and ERK (Kim and Asmis, 2017). Reportedly, curcumin considerably improves sepsis-induced liver injury by inhibiting the JNK/ERK pathway (Zhou et al., 2015). Owing to its structure, THC has better bioavailability and bioactivity than curcumin. Nevertheless, the effects and mechanisms of action of THC in septic cardiomyopathy are yet to be investigated. Thus, we hypothesized that THC might improve cardiac function during sepsis by suppressing oxidative stress and the inflammatory response via the regulation of the JNK/ERK signaling pathway.

Materials and methods

Animal model and treatment

C57BL/6 male mice (8 – 12 weeks old), weighing approximately 25 g, were obtained from the Experimental Animal Center of the Air Force Military Medical University. All animals were housed in cages with a 12 h light/dark cycle at a temperature of 25 °C. The mice were randomly divided into the following groups: control group (Con; $n = 12$), THC-treated Con group (Con+THC; $n = 12$), Sepsis group (Sepsis; $n = 12$), Curcumin-treated Sepsis group (Curcumin+THC; $n = 12$), THC-treated Sepsis group (Sepsis+THC; $n = 12$), THC-treated Sepsis group with NSC95397 supplementation (Sepsis+THC+NSC95397, $n = 12$), and NSC95397-treated group (Sepsis+NSC95397, $n = 12$). We established the sepsis model by intraperitoneally injecting 10 mg/kg lipopolysaccharide (LPS; Sigma Chemical Co., St. Louis, MO, USA). Before LPS injection, THC (a purity of 98% tested by high-performance liquid chromatography) or curcumin (Macklin Biochemical Co. Ltd., Shanghai, China) was administered to normal and septic mice for 5 consecutive days at a dose of 120/100 mg/kg via intragastric administration, as described previously (Li et al., 2019). To regulate the JNK and ERK pathways, the MKP-1 inhibitor NSC95397 (Selleck Chemicals, Houston, TX, USA) was injected intraperitoneally at a dose of 4 mg/kg. Mice from the other groups received the same volume of saline instead. Twelve hours after the LPS injection, myocardial function was assessed and the relevant inflammatory markers were measured to determine the severity of septic cardiomyopathy. All experiments met the requirements of the guidelines for the Care and Use of Laboratory Animals and were approved by the Experimental Animal Ethics Committee of the Air Force Military Medical University.

Cell culture and treatment

H9c2 cells purchased from Tiancheng Technology (Shanghai, China) were cultured in Dulbecco's Modified Eagle Medium (HyClone, Logan, UT, USA) supplemented with 10% fetal bovine serum (Gibco, Grand Island, NY, USA) and 1% penicillin/streptomycin (Sigma, St. Louis, MO, USA) at 37 °C and 5% CO_2. To mimic the *in vivo* conditions, H9c2 cells were also treated with LPS (1 μg/mL), with or without the addition of THC simultaneously. To block MKP-1, cells were transfected with MKP-1 small interfering (si)RNA (Hanbio, Nanjing, Jiangsu, China) for 24 h using Lipofectamine 3000 (Invitrogen, Carlsbad, CA, USA). The cells were assigned to the following groups: PBS-treated group (PBS), THC-treated PBS group (PBS+THC), LPS-treated group (LPS), THC-treated LPS group (LPS+THC), TCH-treated LPS group with the addition of MKP-1 siRNA (LPS+THC+MKP-1 siRNA), and MKP-1 siRNA-treated LPS group (LPS+MKP-1 siRNA). The cells were collected after treatment for 24 h.

Cell viability

Cell viability was assessed using the Cell Counting kit-8 assay (CCK-8; 7Sea Pharmatech Co. Ltd., Shanghai, China) according to the manufacturer's instructions. Briefly, to determine the appropriate concentration of THC, H9c2 cells were seeded in 96-well plates and treated with THC at different concentrations, with or without LPS. After 24 h, 10 μl of CCK-8 solution was added to each well, followed by incubation for 2 h. Viability was determined based on the absorbance at 450 nm, measured via spectrophotometry using the SpectraMax M5 instrument (Molecular Devices, San Jose, CA, USA).

Cardiac function measurements

After anesthetization with 1.0% isoflurane in oxygen, the cardiac function of mice was assessed via transthoracic echocardiography using a linear transducer. Images were obtained with a VisualSonics Vevo 770 ultrasound system (Toronto, Ontario, Canada), as previously described (Zhang et al., 2019). The left ventricular ejection fraction (LVEF) and left ventricular fractional shortening (LVFS) were further calculated using the system software.

Histopathology staining

As previously reported (Zhai et al., 2017), mouse hearts were fixed in 4% paraformaldehyde and then embedded in paraffin. Thereafter, heart tissues were cut into 5 μm thick sections and stained with hematoxylin and eosin to observe changes in the myocardial structure. In addition, immunofluorescence staining of CD68 was employed to identify

macrophage accumulation. Images were acquired using the Olympus FV1000 (Olympus, Tokyo, Japan) laser confocal microscope.

Measurement of ROS

To determine the degree of oxidative stress injury, the intracellular levels of ROS in frozen myocardial tissues and H9c2 cells were measured via staining with dihydroethidium (DHE; Invitrogen) and the fluorescent probe 2′,7′-dichlorofluorescein diacetate (DCFH-DA; Beyotime Institute of Biotechnology, Shanghai, China), respectively, in accordance with the manufacturer's instructions. Images were obtained using the Olympus FV1000 (Olympus) laser confocal microscope, and the fluorescence intensity of ROS in myocardial tissues and cells was determined using Image-Pro 6.0 (Media Cybernetics, Bethesda, MD, USA).

Terminal deoxynucleotidyl transferase dUTP nick-end labeling (TUNEL) assay

Cardiomyocyte apoptosis was assessed via the TUNEL assay using a commercial kit (Roche Molecular Biochemicals, Mannheim, Germany) according to the manufacturer's instructions, as previously described (Xia et al., 2020). Images were obtained using the Olympus FV1000 (Olympus) laser confocal microscope, and the number of apoptotic cells was calculated.

Assessment of myocardial injury and measurement of inflammatory markers

To determine changes in serum myocardial injury and inflammatory markers, the levels of creatine kinase isoenzyme MB (CK-MB), lactate dehydrogenase (LDH), cardiac troponin I (cTnI), TNF-α, and IL-1β were assessed using ELISA kits (Elabscience Biotechnology Co., Ltd., Wuhan, China), in accordance with the manufacturer's instructions. Values were measured via spectrophotometric analysis using the Spectramax M5 instrument (Molecular Devices).

Western blot analysis

As previously described (Zhang et al., 2018), heart tissues and cells were homogenized using RIPA lysis buffer. After centrifugation, the concentration of sample proteins was determined using the bicinchoninic acid protein assay. Proteins were then separated via sodium dodecyl sulfate-polyacrylamide gel electrophoresis and transferred onto a polyvinylidene fluoride membrane. The membranes were blocked using 5% skim milk in Tris-buffered saline with Tween (TBST) at room temperature for 2 h, followed by overnight incubation with primary antibodies at 4 °C. Primary antibodies against phosphorylated JNK (P-JNK, 1:1000), JNK (1:1000), Bax (1:1000), cleaved caspase-3 (1:1000), nuclear factor-erythroid 2-related factor 2 (Nrf2, 1:1000), NAD(P)H quinone oxidoreductase 1 (NQO1, 1:1000), MKP-1 (1:1000), and superoxide dismutase 2 (SOD2, 1:1000) were purchased from Cell Signaling Technology (Beverly, MA, USA). Primary antibodies against phosphorylated ERK (P-ERK, 1:1000), ERK (1:1000), Bcl-2 (1:1000), TNF-α (1:1000), IL-1β (1:1000), and glyceraldehyde-3-phosphate dehydrogenase (GAPDH) (1:1000) were purchased from Proteintech Group (Rosemont, IL, USA). After washing three times in TBST, the membranes were incubated with the rabbit anti-goat or mouse anti-goat secondary antibodies (Zhongshan Company, Beijing, China) for 2 h at room temperature. Finally, the bands were visualized via chemiluminescence, and the density of bands was calculated using Image Lab 5.2.1 (Bio-Rad Laboratories, CA, USA).

Statistical analysis

Data are presented as the mean ± standard error of the mean (SEM) and were analyzed using the GraphPad Prism 8.0 software (GraphPad Software, San Diego, CA, USA). Differences between groups were analyzed via one-way analysis of variance, followed by Tukey's post hoc test for multiple comparisons. $p < 0.05$ was considered to indicate statistical significance.

Results

THC treatment prevented LPS-induced myocardial dysfunction and cardiac injury

As shown in Fig. 1A–C, the echocardiography results indicated that the cardiac systolic function of mice in the Sepsis group was seriously impaired compared to that of mice in the Con group. However, THC treatment alleviated the sepsis-induced decrease in LVEF and LVFS. To assess the effect of THC on cardiac injury, the expression of the classic myocardial injury markers in the serum was analyzed further. THC inhibited the septic cardiomyopathy-associated increase in LDH, CK-MB, and cTnI levels. In addition, THC exerted stronger cardioprotective effects than curcumin. Of note, there was no significant difference between the Con group and the Con+THC group (Fig. 1D–F).

THC attenuated the inflammatory response in sepsis-induced myocardial injury by regulating the JNK/ERK pathway

In the Con group, the myocardial fibers were neatly arranged, and the cardiomyocytes showed an intact morphology. In contrast, a disordered structure was observed in Sepsis group samples. Intriguingly, THC treatment alleviated these adverse changes, as shown in Fig. 2A. To determine the effect of THC on the inflammatory response, CD68 immunofluorescence staining was performed, and the expression of inflammatory cytokines was assessed. Compared with that in the Con group, LPS caused a strong inflammatory response in the myocardium, with macrophage accumulation and an upregulation of inflammatory cytokines, including TNF-α, IL-1β, and IL-6, as indicated by immunofluorescence intensity and the results of ELISA and western blotting, respectively (Figs. 2B, C and 3A–I). As expected, THC markedly attenuated inflammation, with a considerable reduction in inflammatory marker expression as well as a decline in the number of infiltrating macrophages (Fig. 3A–I). Of note, the total levels of JNK and ERK, the upstream molecules mediating the induction of pro-inflammatory cytokine production, in myocardial tissues did not differ between the Con and Sepsis groups. However, their phosphorylated active forms were upregulated under sepsis. Intriguingly, THC supplementation significantly upregulated MKP-1, which is a phosphatase, and decreased the P-JNK/JNK and P-ERK/ERK ratios. These results indicated that THC suppressed the release of inflammatory cytokines via regulation of the JNK/ERK pathway.

THC alleviated oxidative stress injury and cardiomyocyte apoptosis in sepsis

As an imbalance of ROS generation and scavenging is known to occur during sepsis, we assessed the effect of THC on oxidative stress in myocardial tissues. DHE staining revealed that the mice in the Sepsis group had higher myocardial levels of ROS than those in the Con group (Fig. 4A and B). Moreover, oxidative stress-related proteins were analyzed through western blotting to further characterize the THC-mediated inhibition of oxidative stress. The levels of antioxidant markers, including Nrf2, SOD2, and NQO1, were suppressed drastically after LPS injection, in contrast to that in the Con group, in parallel with the upregulation of the prooxidant protein $gp91^{phox}$. However, THC administration reversed these changes (Fig. 4C–G). The loss of cardiomyocytes is one of the major factors contributing to myocardial remodeling and is caused by ROS overproduction. We observed that THC inhibited the sepsis-induced increase in the number of TUNEL-positive cells (Fig. 5A and B). Further, THC treatment not only

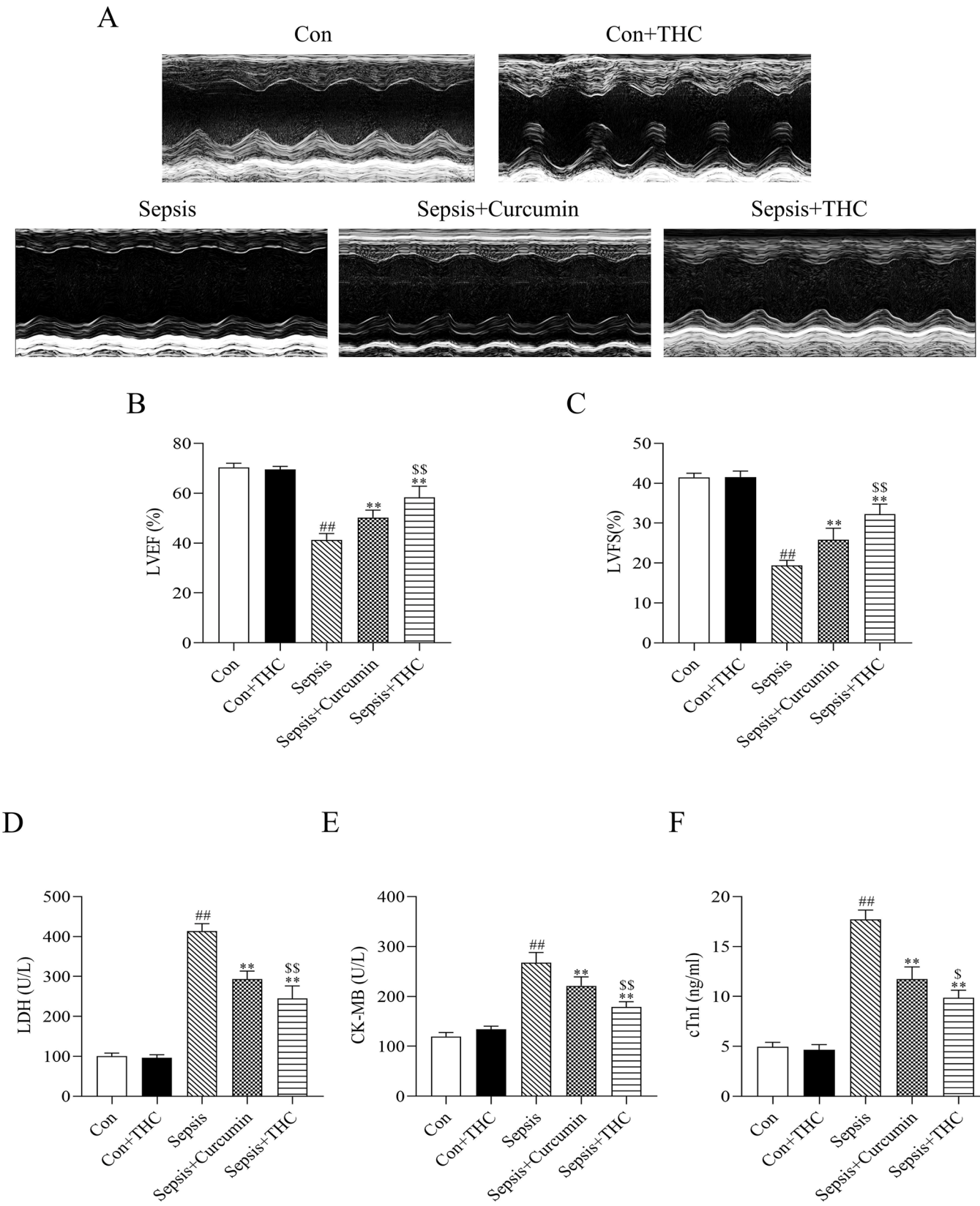

Fig. 1. THC improved cardiac dysfunction and reduced myocardial injury markers expression in septic cardiomyopathy. (A) Representative images of echocardiography. (B) Left ventricular ejection fraction (LVEF). (C) Left ventricular fraction shortening (LVFS). (D–F) Lactate dehydrogenase (LDH), creatine kinase isoenzyme MB (CK-MB), and cardiac troponin I (cTnI) contents in the myocardium, as assessed via ELISA. Data are presented as the mean ± SEM. $n = 5$ in each group. $^{\#\#}p <$ 0.01 versus the Con group; $^{**}p < 0.01$ versus the Sepsis group, $^{\$\$}$ $p < 0.01$ versus the Sepsis+Curcumin group.

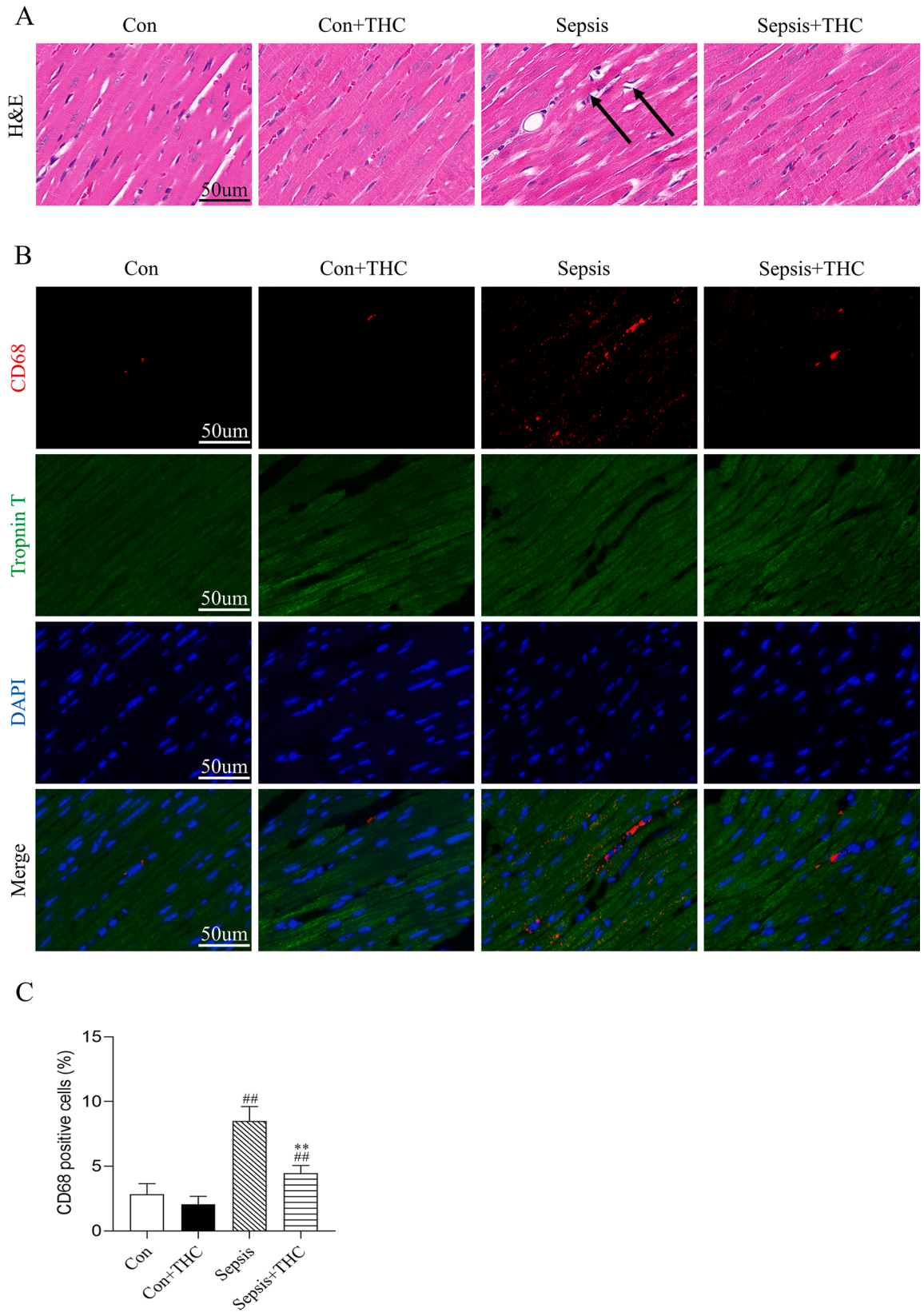

Fig. 2. THC attenuated the adverse myocardial remodeling and macrophages accumulation in the myocardium. (A) H&E staining (the black arrow showed the abnormal myocardial structure, scale bar = 100 μm). (B) Representative images of CD68 immunofluorescence (scale bar = 100 μm). (C) The percentage of CD68 positive cells. Data are presented as the mean ± SEM. $n = 5$ in each group. $^{\#\#}p < 0.01$ versus the Con group; $^{**}p < 0.01$ versus the Sepsis group.

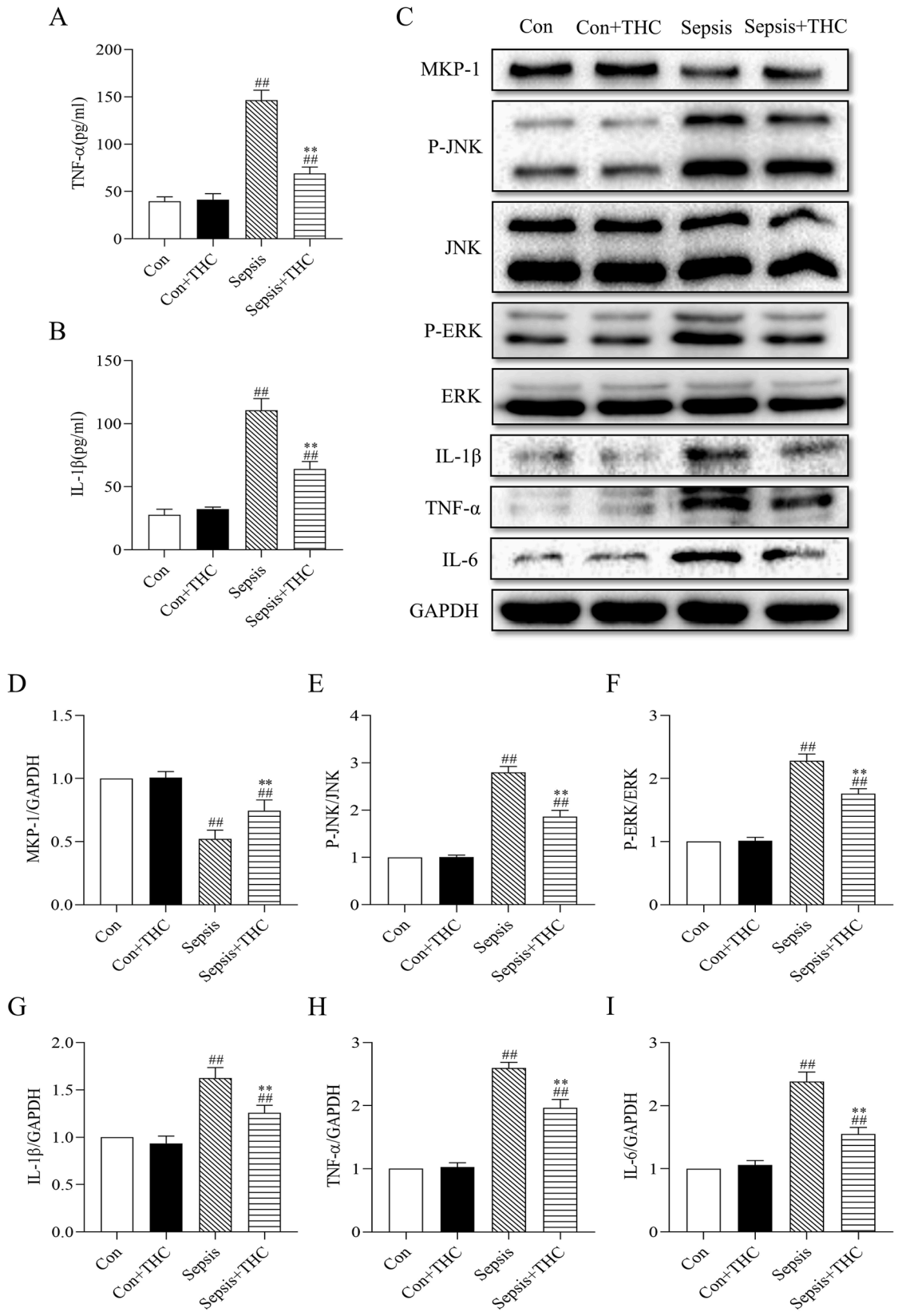

Fig. 3. THC inhibited the expression of IL-1β, TNF-α, and IL-6 by regulating the JNK/ERK signaling pathway. (A-B) The serum level of TNF-α and IL-1β. (C) Representative blots of MKP-1, P-JNK, JNK, P-ERK, ERK, IL-1β, TNF-α and IL-6. (D) Quantitative analysis of the expression of MKP-1. (E) Quantitative analysis of the ratio of P-JNK to JNK. (F) Quantitative analysis of the ratio of P-ERK to ERK. (G–I) Quantitative analysis of the expression of IL-1β, TNF-α, and IL-6. $n = 5$ in each group. $^{\#\#}p < 0.01$ versus the Con group; $^{**}p < 0.01$ versus the Sepsis group.

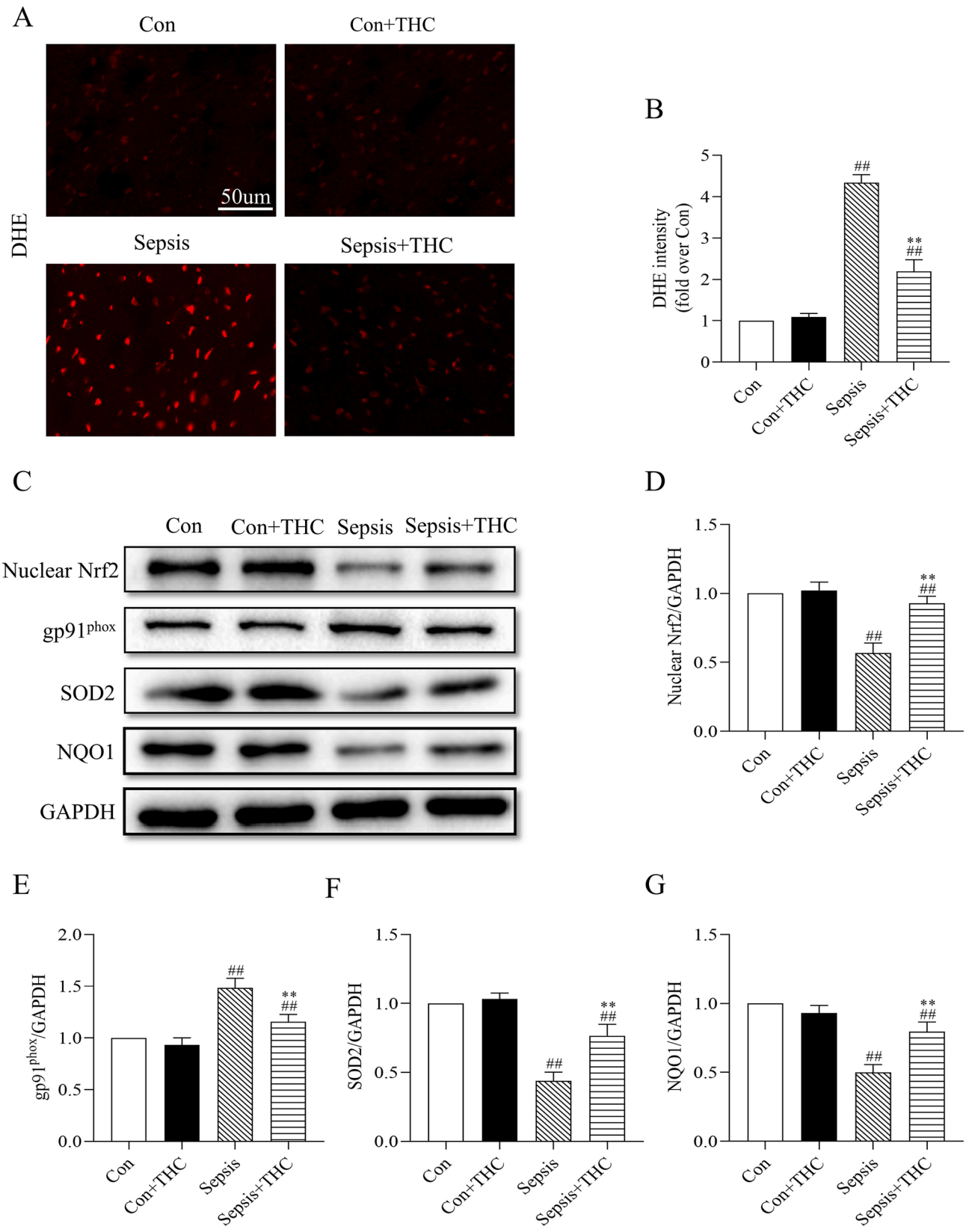

Fig. 4. THC significantly alleviated oxidative stress injury. (A) Representative images of dihydroethidium (DHE) staining (scale bar = 100 μm). (B) DHE intensity. (C) Representative blots of Nuclear Nrf2, gp91^{phox}, SOD2, and NQO1. (D–G) Quantitative analysis of the expression of Nuclear Nrf2, gp91^{phox}, SOD2, and NQO1. $n = 5$ in each group. $^{\#\#}p < 0.01$ versus the Con group; $^{**}p < 0.01$ versus the Sepsis group.

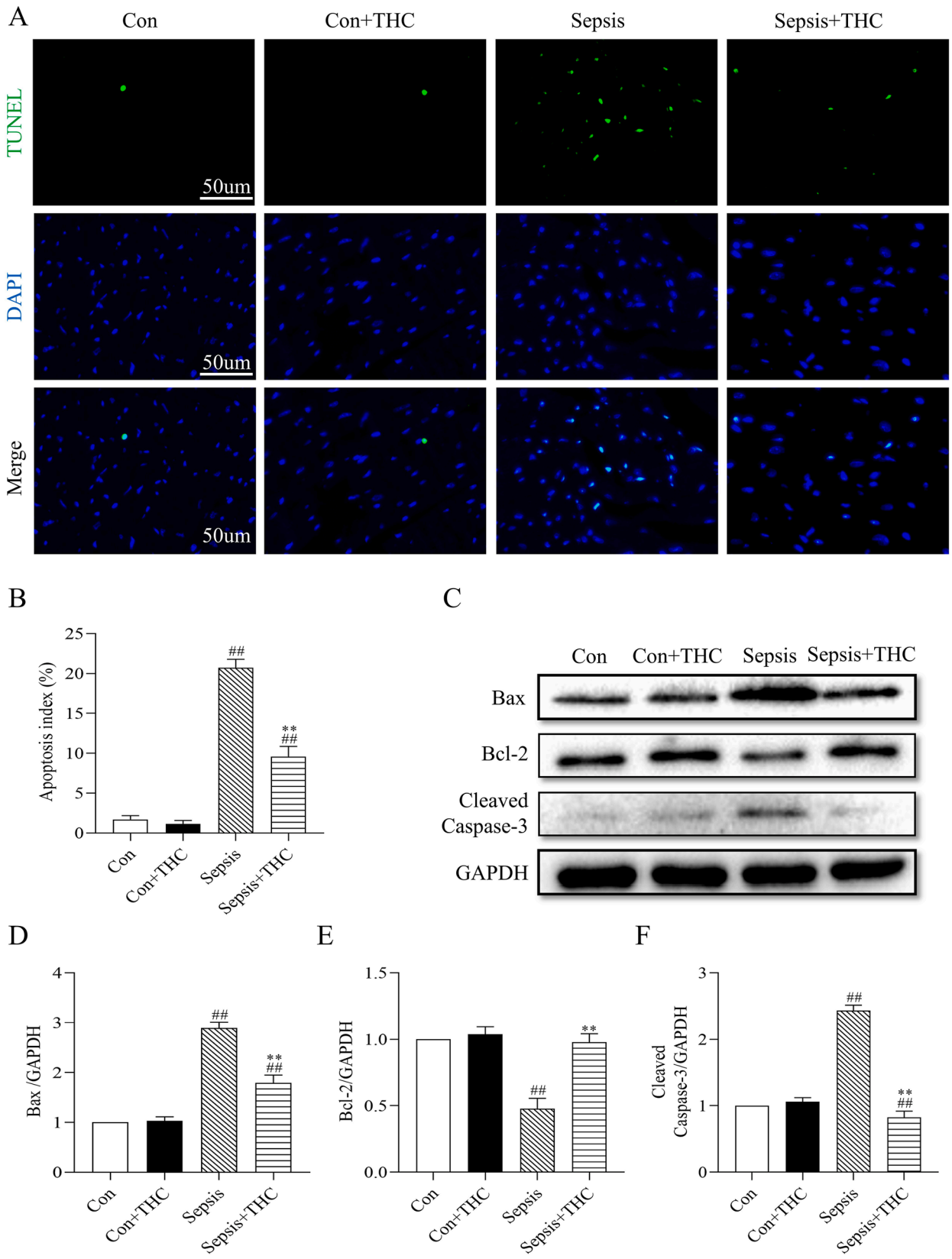

Fig. 5. THC suppressed cardiomyocyte apoptosis in septic cardiomyopathy. (A) Representative images of TUNEL assay (scale bar = 100 μm). (B) The proportion of apoptotic cells. (C) Representative blots of Bax, Bcl-2, and cleaved caspase-3. (D–F) Quantitative analysis of the expression of Bax, Bcl-2, and cleaved caspase-3. $n = 5$ in each group. $^{\#\#}p < 0.01$ versus the Con group; $^{**}p < 0.01$ versus the Sepsis group.

downregulated the expression of proapoptotic proteins, including Bax and cleaved caspase-3, but also enhanced that of the antioxidant protein Bcl-2, during septic cardiomyopathy (Fig. 5C–F). In addition, no difference in the expression of these proteins was observed between the Con and Con+THC groups. These data demonstrated that THC attenuated oxidative stress and cardiomyocyte apoptosis in sepsis-induced myocardial injury.

THC blocked LPS-induced inflammation by regulating the JNK/ERK pathway in H9c2 cells

After the results of our *in vivo* experiment were obtained, we investigated whether THC could exert similar effects on H9c2 cells stimulated with LPS. The CCK-8 assay was employed to determine the appropriate THC concentration for the treatment of H9c2 cells. THC concentrations less than 10 μg/mL did not cause toxicity in normal cultured H9c2 cells. Additionally, THC at a concentration of 4 μg/mL exerted the strongest effect in improving LPS-induced H9c2 cell injury (Fig. 6A and B). As anticipated in the LPS group, inflammatory markers, such as TNF-α, IL-1β, and IL-6, were considerably upregulated. The addition of THC suppressed the levels of inflammatory cytokines, as confirmed via western blotting (Fig. 6C–F). Furthermore, THC effectively activated MKP-1 and subsequently suppressed the LPS-induced phosphorylation of JNK and ERK, confirming the suppression of cardiomyocyte inflammation as its mechanism of action (Fig. 6G–I).

THC ameliorated LPS-induced ros overproduction and apoptosis in H9c2 cells

Compared to that in the PBS group, LPS drastically increased the intracellular ROS levels, whereas THC administration limited ROS overproduction, as indicated by the intensity of DCFH-DA fluorescence (Fig. 7A and B). In agreement with the *in vivo* results, THC upregulated the protein expression of Nrf2, SOD2, and NQO1, while suppressing $gp91^{phox}$ expression in LPS-treated H9c2 cells (Fig. 7C–G). As shown in Fig. 8A and B, the results of the TUNEL assay indicated that THC suppressed the LPS-induced increase in apoptosis. Consistent with the *in vivo* results, the LPS-induced increase in Bax and cleaved caspase-3 expression as well as the decrease in Bcl-2 expression were reversed by THC treatment (Fig. 8C–F).

THC regulated the jnk/erk pathway by activating MKP-1

To further explore the mechanism underlying the effect of THC on JNK and ERK dephosphorylation, we administered the MKP-1 inhibitor NSC95037 and siRNA to promote phosphorylation. The inhibition of MKP-1 expression markedly diminished the cardioprotective effect of THC on sepsis, as shown in Supplementary Fig. 1A–F. Additionally, NSC95037 significantly inhibited the anti-inflammatory and anti-apoptotic effects of THC (Fig. 9A–I). Of note, the decrease in phosphorylated JNK and ERK protein expression and the increase in MKP-1 expression in mice with sepsis treated with THC were also inhibited by NSC95037 (Fig. 9C–F). In line with the *in vivo* results, MKP-1 siRNA also suppressed JNK/ERK dephosphorylation and the low ratio of cardiomyocyte apoptosis in LPS-treated H9c2 cells under THC treatment (Supplementary Figs. 2A–B and 3A–G).

Discussion

Our current findings provide evidence of the protective effects of the medicinal compound THC against sepsis-induced myocardial dysfunction. Changes in myocardial systolic function were reversed by THC treatment, as was the damage to cardiac structure. Furthermore, THC markedly suppressed the production of inflammatory cytokines, including TNF-α, IL-1β, and IL-6, through the inhibition of ERK and JNK phosphorylation in both the sepsis mouse model and LPS-treated H9c2 cells. Additionally, THC played a crucial role in limiting ROS generation and elevating antioxidant protein expression. Collectively, our results suggest the favorable effects of THC against septic cardiomyopathy.

Most sepsis-causing infections are attributed to LPS, which is a component of the gram-negative bacterial cell wall and an endotoxin (Downs et al., 2020). The accumulation of LPS activates Toll-like receptors to trigger an inflammatory response (Romerio and Peri, 2020). Thus, the septic cardiomyopathy model is always established via LPS injection, as previously described (Ndongson Dongmo et al., 2019). In this study, LPS compromised the cardiac contractile function, as indicated by the low LVEF and LVFS. Furthermore, the levels of myocardial injury markers and inflammatory cytokines were elevated in the serum and myocardium, respectively. The *in vitro* experiment showed that the viability of H9c2 cells was decreased and accompanied by the upregulation of inflammatory protein expression, indicating the successful establishment of the sepsis model.

THC is a major metabolite of curcumin, with similar effects reported in multiple cardiovascular diseases (Mahattanadul et al., 2020; Liu et al., 2017). THC has been proven to prevent the development of cardiac hypertrophy, myocardial infarction, and diabetic cardiomyopathy (Li et al., 2019; Lau et al., 2018; Ali et al., 2009). In addition, several studies have reported that THC exerts multiple effects on inflammation, oxidative stress, and apoptosis (Wu et al., 2020; Trivedi et al., 2020). However, as no report has been published on the protective effects of THC against septic cardiomyopathy, we designed the current study to explore these. In this study, we clearly demonstrated that THC supplementation alleviated LPS-induced cardiac dysfunction and cardiomyocyte injury, while it decreased the levels of CK-MB, LDH, and cTnI, and we found that the beneficial effects of THC on septic cardiomyopathy might be related to inflammation and oxidative stress. During sepsis, the inflammatory response is one of the major processes leading to acute myocardial damage. An increasing number of macrophages is recruited into the myocardium, wherein they secrete pro-inflammatory cytokines, including TNF-α and IL-6, in excess, as shown in LPS-treated mice (Huang et al., 2018). Based on findings from published literature, THC administration prevents the development of osteoarthritis symptoms, and this effect is associated with the downregulation of TNF-α, IL-1β, and IL-6 expression (Park et al., 2016). Similarly, our data suggested that THC markedly reversed the LPS-stimulated increase in inflammatory factor expression and reduced macrophage accumulation in myocardial tissues. It is generally accepted that the MAPK signaling pathway chiefly mediates the inflammatory response in sepsis (Peng et al., 2009). The neuroprotective effects of THC mediated via MAPK pathway regulation have been reported previously; however, limited information is available regarding its mechanisms of action against cardiomyopathy. Lin et al. reported that the intraperitoneal injection of THC suppressed the phosphorylation of ERK in cerebral ischemia/reperfusion injury (Lin et al., 2016). Moreover, THC treatment downregulated JNK and ERK phosphorylation in glutamate-induced HT22 cell injury (Park et al., 2019). Consistent with the findings from these studies, the results of our study indicated that the phosphorylation of ERK and JNK was considerably elevated in the sepsis mouse model and LPS-treated H9c2 cells. More importantly, THC limited JNK and ERK phosphorylation by activating MKP-1, thus downregulating downstream inflammatory cytokine production. These findings confirmed that THC could significantly attenuate the sepsis-induced inflammatory response via JNK/ERK pathway regulation.

In addition to the inflammatory response, oxidative stress injury is an essential trigger of myocardial injury in sepsis, as the latter is characterized by ROS overproduction (Yim et al., 2020). Excessive ROS enhance cellular oxidative stress by reacting with proteins, DNA, and lipids, inducing a series of responses in cardiomyocytes, including apoptosis, autophagy, and pyroptosis. Therefore, suppressing ROS production is crucial for the treatment of sepsis (Regmi et al., 2020; Li et al., 2019). Findings from numerous studies have demonstrated the ability of THC to limit ROS production in various diseases (Sangartit et al., 2016;

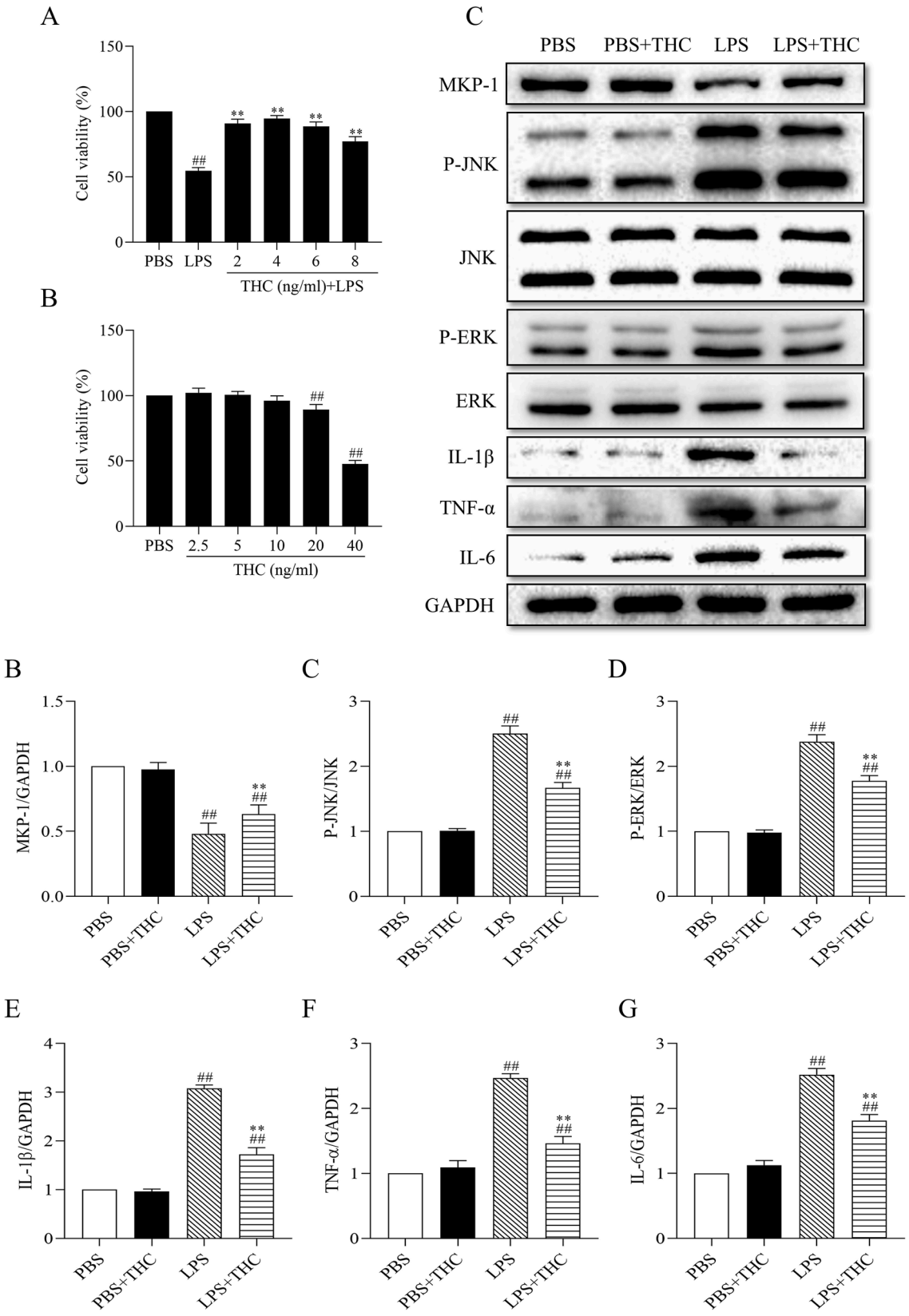

Fig. 6. THC protected H9c2 cells injury by suppressing inflammation via JNK/ERK signaling pathway regulation. (A) THC had no significant effect on normal H9c2 cells at a concentration of 20 μg/ml. (B) THC notably improved cell viability under LPS stimulation at the dose of 4 μg/ml. (C) Representative blots of MKP-1, P-JNK, JNK, P-ERK, ERK, IL-1β, TNF-α, IL-6, and GAPDH. (D) Quantitative analysis of the expression of MKP-1. (E) Quantitative analysis of the ratio of P-JNK to JNK. (F) Quantitative analysis of the ratio of P-ERK to ERK. (G–I) Quantitative analysis of the expression of IL-1β, TNF-α, and IL-6. $n = 5$ or 6 in each group. $^{\#\#}p < 0.01$ versus the PBS group; $^{**}p < 0.01$ versus the LPS group.

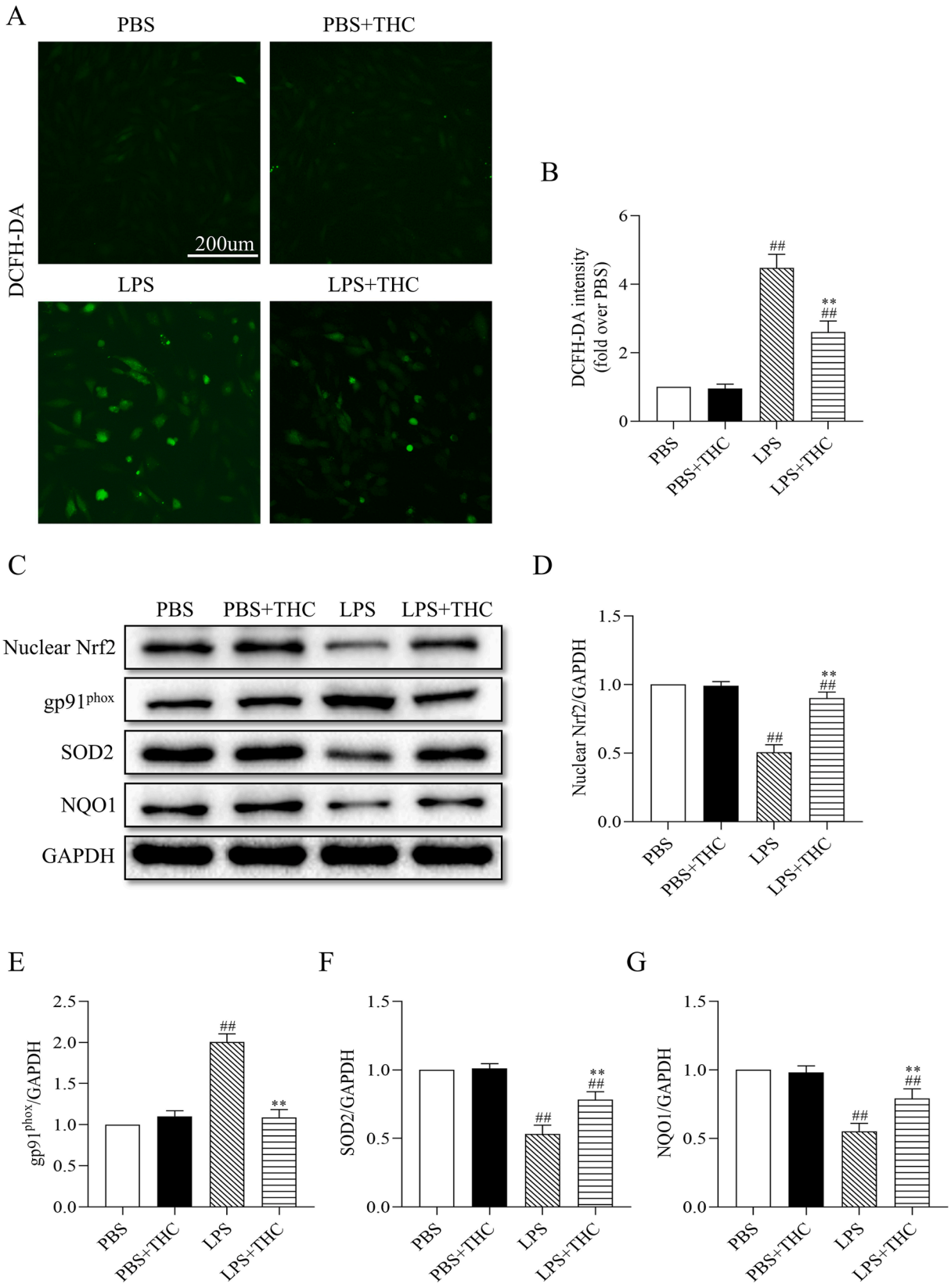

Fig. 7. THC attenuated the LPS-induced oxidative stress injury in H9c2 cells. (A) Representative images of DCFH-DA staining (scar bar = 200 μm). (B) DCFH-DA intensity. (C) Representative blots of Nuclear Nrf2, gp91^{phox}, SOD2, and NQO1. (D–G) Quantitative analysis of Nuclear Nrf2, gp91^{phox}, SOD2, and NQO1 expression. $n = 5$ in each group. $^{\#\#}p < 0.01$ versus the PBS group; $^{**}p < 0.01$ versus the LPS group.

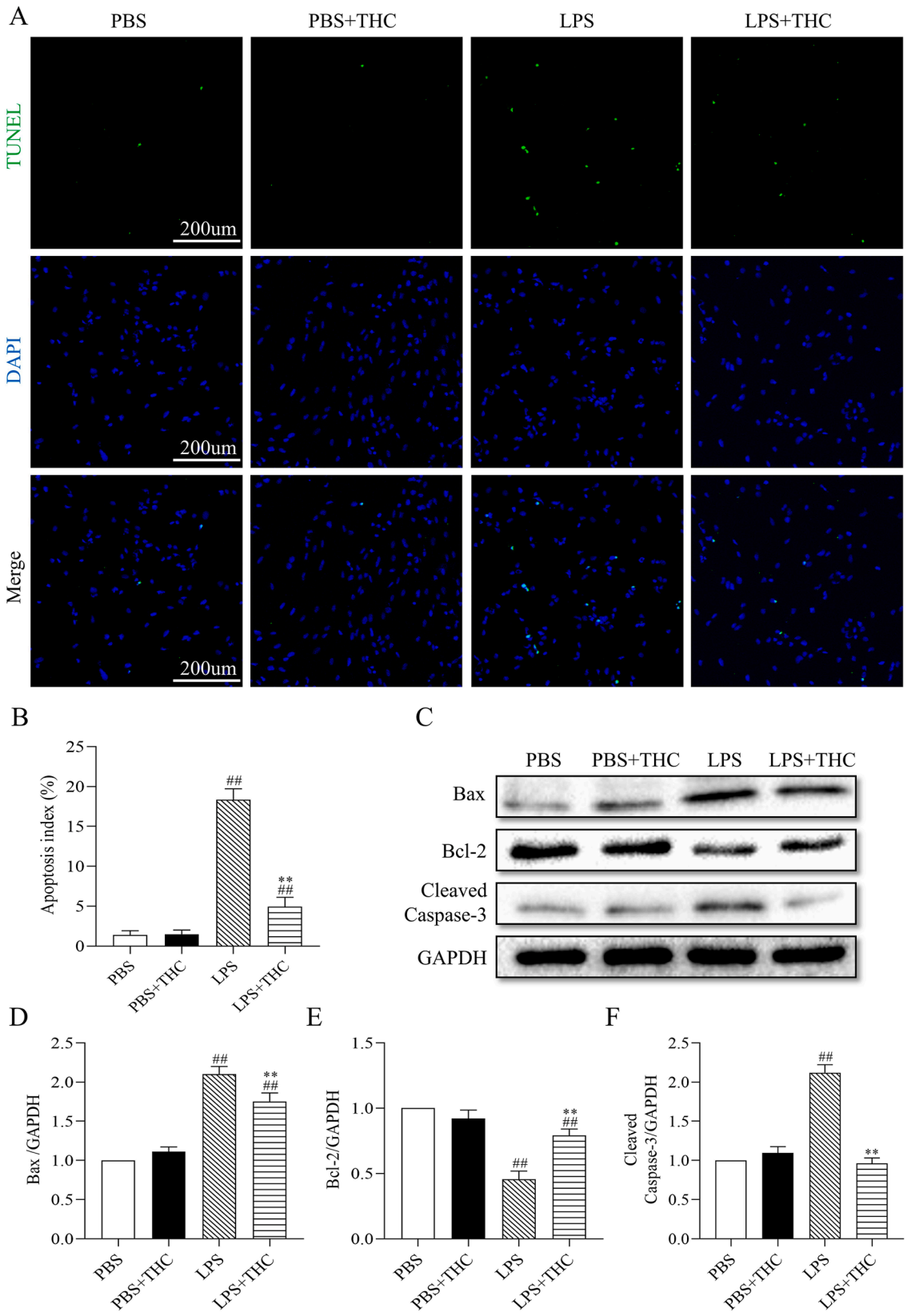

Fig. 8. THC suppressed apoptosis in LPS-treated H9c2 cells. (A) Representative images of TUNEL assay (scale bar = 200 μm). (B) The proportion of apoptotic cells. (C) Representative blots of Bax, Bcl-2, and cleaved caspase-3. (D–F) Quantitative analysis of Bax, Bcl-2, and cleaved caspase-3 expression. $n = 5$ in each group. $^{\#\#}p < 0.01$ versus the PBS group; $^{**}p < 0.01$ versus the LPS group.

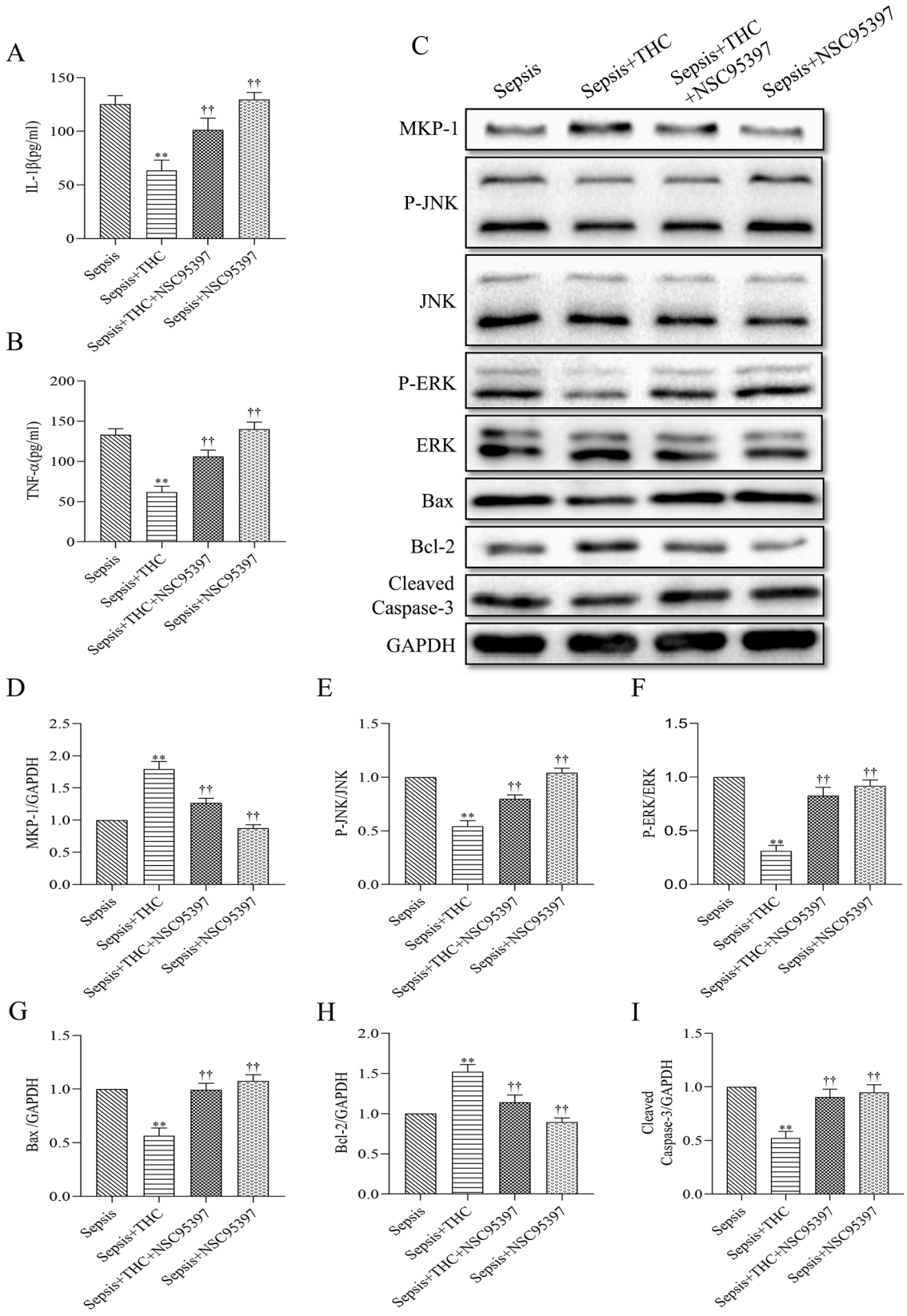

Fig. 9. THC dephosphorylated JNK and ERK via activating MKP-1. (A-B) The serum levels of TNF-α and IL-1β. (C) Representative blots of MKP-1, P-JNK, JNK, P-ERK, ERK, Bax, Bcl-2 and Cleaved Caspase-3. (D) Quantitative analysis of the expression of MKP-1. (E) Quantitative analysis of the ratio of P-JNK to JNK. (F) Quantitative analysis of the ratio of P-ERK to ERK. (G–I) Quantitative analysis of the expression of Bax, Bcl-2 and Cleaved Caspase-3. $n = 5$ in each group. $^{**}p < 0.01$ versus the Sepsis group; $^{\dagger\dagger}p < 0.01$ versus the Sepsis+THC group.

Vacek et al., 2018). Gao et al. found that THC treatment reduced malondialdehyde content and enhanced glutathione peroxidase activity, as well as our previous results in diabetic cardiomyopathy (Li et al., 2019; Gao et al., 2017). In this study, the ROS levels in myocardial tissues and H9c2 cells increased upon LPS treatment; however, these changes were reversed by THC. The specific effect of THC on oxidative stress-related molecules was further determined. Nrf2, an important antioxidant sensor, plays an essential role against oxidative stress injury, and its activation enhances the expression of genes encoding antioxidant enzymes, including SOD2 and NQO1, as confirmed from our previous data (Zhang et al., 2019). Additionally, THC has been proven to activate Nrf2 in acetaminophen-induced liver injury (Luo et al., 2019). Here, our results revealed that THC significantly inhibited the decrease in Nrf2 expression and upregulated SOD2 and NQO1 expression, while suppressing $gp91^{phox}$ expression, in septic cardiomyopathy as well as in LPS-treated H9c2 cells. These observations confirmed the efficacy of THC in alleviating oxidative stress damage.

Cardiomyocyte apoptosis is one of the final stages in septic cardiomyopathy and is induced by inflammation and oxidative stress (Jia et al., 2018). The number of cardiomyocytes is closely associated with myocardial systolic function; thus, cardiomyocyte apoptosis contributes to cardiac failure. In the neural system, the protective effects of THC against neuronal injury were primarily attributed to the inhibition of apoptosis (Wei et al., 2017). In line with these observations, our results revealed that THC reversed the LPS-induced increase in the number of TUNEL-positive cells as well as in Bax upregulation and cleaved caspase-3 expression and the decrease in Bcl-2 expression. Taken together, the anti-apoptotic effects of THC in septic cardiomyopathy contribute to the recovery of cardiac function, and THC will be a promising drug for the treatment of sepsis in future.

Conclusion

In summary, our results suggest that THC markedly improves cardiac dysfunction during sepsis by inhibiting inflammation, oxidative stress, and cardiomyocyte apoptosis through the regulation of the JNK/ERK signaling pathway. Nevertheless, this study had some limitations; the exact molecular mechanisms require further elucidation for determining the potential of THC as a drug against septic cardiomyopathy.

Funding

This study was financially supported by the National Natural Science Foundation of China (grant numbers 81770373, 81870218, 82070503).

CRediT authorship contribution statement

Hanzhao Zhu: Writing – original draft, Writing – review & editing. **Liyun Zhang:** Writing – original draft, Writing – review & editing. **Hao Jia:** Writing – original draft, Writing – review & editing. **Lu Xu:** Writing – original draft. **Yu Cao:** Supervision. **Mengen Zhai:** Methodology, Supervision. **Kaifeng Li:** Writing – review & editing. **Lin Xia:** Writing – original draft. **Liqing Jiang:** . **Xiang Li:** Methodology. **Yenong Zhou:** Supervision. **Jincheng Liu:** Methodology. **Shiqiang Yu:** Conceptualization, Supervision, Funding acquisition. **Weixun Duan:** Conceptualization, Supervision, Project administration, Funding acquisition.

Declaration of Competing Interest

The authors declare that there is no conflict of interest regarding the publication of this paper.

Supplementary materials

Supplementary material associated with this article can be found, in the online version, at doi:10.1016/j.phymed.2022.154283.

References

Ali, M.S., Mudagal, M.P., Goli, D., 2009. Cardioprotective effect of tetrahydrocurcumin and rutin on lipid peroxides and antioxidants in experimentally induced myocardial infarction in rats. Pharmazie 64, 132–136.
Caraballo, C., Jaimes, F., 2019. Organ dysfunction in sepsis–An ominous trajectory from infection to death. Yale J. Biol. Med. 92, 629–640.
Chen, B.L., Chen, Y.Q., Ma, B.H., Yu, S.F., Li, L.Y., Zeng, Q.X., Zhou, Y.T., Wu, Y.F., Liu, W.L., Wan, J.B., Yang, Y., Li, C.W., 2018. Tetrahydrocurcumin, a major metabolite of curcumin, ameliorates allergic airway inflammation by attenuating Th2 response and suppressing the IL-4Ralpha-Jak1-STAT6 and Jagged1/Jagged2 -Notch1/Notch2 pathways in asthmatic mice. Clin. Exp. Allergy 48, 1494–1508.
Downs, K.P., Nguyen, H., Dorfleutner, A., Stehlik, C., 2020. An overview of the non-canonical inflammasome. Mol. Aspects Med. 76, 100924.
Fleischmann, C., Scherag, A., Adhikari, N.K., Hartog, C.S., Tsaganos, T., Schlattmann, P., Angus, D.C., Reinhart, K., 2016. Assessment of global incidence and mortality of hospital-treated sepsis. Current estimates and limitations. Am. J. Respir. Crit. Care Med. 193, 259–272.
Flynn, A., Chokkalingam, M.B., Mather, P.J., 2010. Sepsis-induced cardiomyopathy–a review of pathophysiologic mechanisms. Heart Fail. Rev. 15, 605–611.
Gao, Y., Zhuang, Z., Gao, S., Li, X., Zhang, Z., Ye, Z., Li, L., Tang, C., Zhou, M., Han, X., Li, J., 2017. Tetrahydrocurcumin reduces oxidative stress-induced apoptosis via the mitochondrial apoptotic pathway by modulating autophagy in rats after traumatic brain injury. Am. J. Transl. Res. 9, 887–899.
Huang, S.H., Xu, M., Wu, H.M., Wan, C.X., Wang, H.B., Wu, Q.Q., Liao, H.H., Deng, W., Tang, Q.Z., 2018. Isoquercitrin attenuated cardiac dysfunction Via AMPKalpha-dependent pathways in LPS-treated mice. Mol. Nutr. Food Res. 62, e1800955.
Huang, C.Y., Lai, C.H., Kuo, C.H., Chiang, S.F., Pai, P.Y., Lin, J.Y., Chang, C.F., Viswanadha, V.P., Kuo, W.W., Huang, C.Y., 2018. Inhibition of ERK-Drp1 signaling and mitochondria fragmentation alleviates IGF-IIR-induced mitochondria dysfunction during heart failure. J. Mol. Cell. Cardiol. 122, 58–68.
Jia, L., Wang, Y., Wang, Y., Ma, Y., Shen, J., Fu, Z., Wu, Y., Su, S., Zhang, Y., Cai, Z., Wang, J., Xiang, M., 2018. Heme oxygenase-1 in macrophages drives septic cardiac dysfunction via suppressing lysosomal degradation of inducible nitric oxide synthase. Circ. Res. 122, 1532–1544.
Lv, X., Wang, H., 2016. Pathophysiology of sepsis-induced myocardial dysfunction. Mil. Med. Res. 3, 30.
Li, K., Zhai, M., Jiang, L., Song, F., Zhang, B., Li, J., Li, H., Li, B., Xia, L., Xu, L., Cao, Y., He, M., Zhu, H., Zhang, L., Liang, H., Jin, Z., Duan, W., Wang, S., 2019. Tetrahydrocurcumin ameliorates diabetic cardiomyopathy by attenuating high glucose-induced oxidative stress and fibrosis via activating the SIRT1 pathway. Oxid. Med. Cell. Longev., 6746907
Luo, D.D., Chen, J.F., Liu, J.J., Xie, J.H., Zhang, Z.B., Gu, J.Y., Zhuo, J.Y., Huang, S., Su, Z.R., Sun, Z.H., 2019. Tetrahydrocurcumin and octahydrocurcumin, the primary and final hydrogenated metabolites of curcumin, possess superior hepatic-protective effect against acetaminophen-induced liver injury–role of CYP2E1 and Keap1-Nrf2 pathway. Food Chem. Toxicol. 123, 349–362.
Liu, W., Zhang, Z., Lin, G., Luo, D., Chen, H., Yang, H., Liang, J., Liu, Y., Xie, J., Su, Z., Cao, H., 2017. Tetrahydrocurcumin is more effective than curcumin in inducing the apoptosis of H22 cells via regulation of a mitochondrial apoptosis pathway in ascites tumor-bearing mice. Food Funct. 8, 3120–3129.
Kim, H.S., Asmis, R., 2017. Mitogen-activated protein kinase phosphatase 1 (MKP-1) in macrophage biology and cardiovascular disease. A redox-regulated master controller of monocyte function and macrophage phenotype. Free Radic. Biol. Med. 109, 75–83.
Lau, W.L., Khazaeli, M., Savoj, J., Manekia, K., Bangash, M., Thakurta, R.G., Dang, A., Vaziri, N.D., Singh, B., 2018. Dietary tetrahydrocurcumin reduces renal fibrosis and cardiac hypertrophy in 5/6 nephrectomized rats. Pharmacol. Res. Perspect. 6, e00385.
Lin, B., Yu, H., Lin, Y., Cai, C., Lu, H., Zhu, X., 2016. Suppression of GRASP65 phosphorylation by tetrahydrocurcumin protects against cerebral ischemia/reperfusion injury via ERK signaling. Mol. Med. Rep. 14, 4775–4780.
Li, N., Zhou, H., Wu, H., Wu, Q., Duan, M., Deng, W., Tang, Q., 2019. STING-IRF3 contributes to lipopolysaccharide-induced cardiac dysfunction, inflammation, apoptosis and pyroptosis by activating NLRP3. Redox Biol. 24, 101215.
Mantzarlis, K., Tsolaki, V., Zakynthinos, E., 2017. Role of oxidative stress and mitochondrial dysfunction in sepsis and potential therapies. Oxid. Med. Cell. Longev. 2017, 5985209, 2017.
Mahattanadul, S., Kongpuckdee, S., Wiwattanapatapee, R., Tansakul, P., Nitiruangjaras, A., Hansakul, P., 2020. Comparative inhibitory efficacy on the iNOS/NO system of curcumin- and tetrahydrocurcumin-self-microemulsifying liquid formulation in chronic gastric ulcer model. Curr. Pharm. Biotechnol.
Ndongson-Dongmo, B., Lang, G.P., Mece, O., Hechaichi, N., Lajqi, T., Hoyer, D., Brodhun, M., Heller, R., Wetzker, R., Franz, M., Levy, F.O., Bauer, R., 2019. Reduced ambient temperature exacerbates SIRS-induced cardiac autonomic dysregulation and myocardial dysfunction in mice. Basic Res. Cardiol. 114, 26.
Parrillo, J.E., Parker, M.M., Natanson, C., Suffredini, A.F., Danner, R.L., Cunnion, R.E., Ognibene, F.P., 1990. Septic shock in humans. Advances in the understanding of pathogenesis, cardiovascular dysfunction, and therapy. Ann. Intern. Med. 113, 227–242.
Park, S., Lee, L.R., Seo, J.H., Kang, S., 2016. Curcumin and tetrahydrocurcumin both prevent osteoarthritis symptoms and decrease the expressions of pro-inflammatory cytokines in estrogen-deficient rats. Genes Nutr. 11, 2.
Park, C.H., Song, J.H., Kim, S.N., Lee, J.H., Lee, H.J., Kang, K.S., Lim, H.H., 2019. Neuroprotective effects of tetrahydrocurcumin against glutamate-induced oxidative stress in hippocampal HT22 cells. Molecules. 25, 144.

Pan, Y., Zhang, Y., Yuan, J., Ma, X., Zhao, Y., Li, Y., Li, F., Gong, X., Zhao, J., Tang, H., Wang, J., 2020. Tetrahydrocurcumin mitigates acute hypobaric hypoxia-induced cerebral oedema and inflammation through the NF-kappaB/VEGF/MMP-9 pathway. Phytother. Res. 34, 2963–2977.

Peng, T., Zhang, T., Lu, X., Feng, Q., 2009. JNK1/c-fos inhibits cardiomyocyte TNF-alpha expression via a negative crosstalk with ERK and p38 MAPK in endotoxaemia. Cardiovasc. Res. 81, 733–741.

Romerio, A., Peri, F., 2020. Increasing the chemical variety of small-molecule-based TLR4 modulators–an overview. Front. Immunol. 11, 1210.

Regmi, S., Raut, P.K., Pathak, S., Shrestha, P., Park, P.H., Jeong, J.H., 2020. Enhanced viability and function of mesenchymal stromal cell spheroids is mediated via autophagy induction. Autophagy 17, 2991–3010.

Suzuki, T., Suzuki, Y., Okuda, J., Kurazumi, T., Suhara, T., Ueda, T., Nagata, H., Morisaki, H., 2017. Sepsis-induced cardiac dysfunction and beta-adrenergic blockade therapy for sepsis. J. Intensive Care 5, 22.

Sato, K., Kadiiska, M.B., Ghio, A.J., Corbett, J., Fann, Y.C., Holland, S.M., Thurman, R.G., Mason, R.P., 2002. *In vivo* lipid-derived free radical formation by NADPH oxidase in acute lung injury induced by lipopolysaccharide–a model for ARDS. FASEB J. 16, 1713–1720.

Song, Z., Zhang, Y., Zhang, H., Rajendran, R.S., Wang, R., Hsiao, C.D., Li, J., Xia, Q., Liu, K., 2020. Isoliquiritigenin triggers developmental toxicity and oxidative stress-mediated apoptosis in zebrafish embryos/larvae via Nrf2-HO1/JNK-ERK/mitochondrion pathway. Chemosphere 246, 125727.

Sangartit, W., Pakdeechote, P., Kukongviriyapan, V., Donpunha, W., Shibahara, S., Kukongviriyapan, U., 2016. Tetrahydrocurcumin in combination with deferiprone attenuates hypertension, vascular dysfunction, baroreflex dysfunction, and oxidative stress in iron-overloaded mice. Vasc. Pharmacol. 87, 199–208.

Trivedi, M.K., Panda, P., Sethi, K.K., Gangwar, M., Mondal, S.C., Jana, S., 2020. Solid and liquid state characterization of tetrahydrocurcumin using XRPD, FT-IR, DSC, TGA, LC-MS, GC–MS, and NMR and its biological activities. J. Pharm. Anal. 10, 334–345.

Vieillard-Baron, A., Caille, V., Charron, C., Belliard, G., Page, B., Jardin, F., 2008. Actual incidence of global left ventricular hypokinesia in adult septic shock. Crit. Care Med. 36, 1701–1706.

Vacek, J.C., Behera, J., George, A.K., Kamat, P.K., Kalani, A., Tyagi, N., 2018. Tetrahydrocurcumin ameliorates homocysteine-mediated mitochondrial remodeling in brain endothelial cells. J. Cell. Physiol. 233, 3080–3092.

Wu, Y.F., Chen, Y.Q., Li, Q., Ye, X.Y., Zuo, X., Shi, Y.L., Guo, X.Y., Xu, L., Sun, L., Li, C.W., Yang, Y., 2020. Supplementation with tetrahydrocurcumin enhances the therapeutic effects of dexamethasone in a murine model of allergic asthma. Int. Arch. Allergy Immunol. 181, 822–830.

Wei, G., Chen, B., Lin, Q., Li, Y., Luo, L., He, H., Fu, H., 2017. Tetrahydrocurcumin provides neuroprotection in experimental traumatic brain injury and the Nrf2 signaling pathway as a potential mechanism. Neuroimmunomodulat 24, 348–355.

Xie, S., Liu, B., Fu, S., Wang, W., Yin, Y., Li, N., Chen, W., Liu, J., Liu, D., 2014. GLP-2 suppresses LPS-induced inflammation in macrophages by inhibiting ERK phosphorylation and NF-kappaB activation. Cell. Physiol. Biochem. 34, 590–602.

Xia, L., Sun, C., Zhu, H., Zhai, M., Zhang, L., Jiang, L., Hou, P., Li, J., Li, K., Liu, Z., Li, B., Wang, X., Yi, W., Liang, H., Jin, Z., Yang, J., Yi, D., Liu, J., Yu, S., Duan, W., 2020. Melatonin protects against thoracic aortic aneurysm and dissection through SIRT1-dependent regulation of oxidative stress and vascular smooth muscle cell loss. J. Pineal Res. 69, e12661.

Yim, D., Lee, D.E., So, Y., Choi, C., Son, W., Jang, K., Yang, C.S., Kim, J.H., 2020. Sustainable nanosheet antioxidants for sepsis therapy via scavenging intracellular reactive oxygen and nitrogen species. ACS Nano 14, 10324–10336.

Zhang, Z.B., Luo, D.D., Xie, J.H., Xian, Y.F., Lai, Z.Q., Liu, Y.H., Liu, W.H., Chen, J.N., Lai, X.P., Lin, Z.X., Su, Z.R., 2018. Curcumin's metabolites, tetrahydrocurcumin and octahydrocurcumin, possess superior anti-inflammatory effects in vivo through suppression of TAK1-NF-kappaB pathway. Front. Pharmacol. 9, 1181.

Zhou, Y., Zhang, T., Wang, X., Wei, X., Chen, Y., Guo, L., Zhang, J., Wang, C., 2015. Curcumin modulates macrophage polarization through the inhibition of the toll-like receptor 4 expression and its signaling pathways. Cell. Physiol. Biochem. 36, 631–641.

Zhang, B., Zhai, M., Li, B., Liu, Z., Li, K., Jiang, L., Zhang, M., Yi, W., Yang, J., Yi, D., Liang, H., Jin, Z., Duan, W., Yu, S., 2019. Honokiol ameliorates myocardial ischemia/reperfusion injury in type 1 diabetic rats by reducing oxidative stress and apoptosis through activating the SIRT1-Nrf2 signaling pathway. Oxid. Med. Cell. Longev., 3159801

Zhai, M., Liu, Z., Zhang, B., Jing, L., Li, B., Li, K., Chen, X., Zhang, M., Yu, B., Ren, K., Yang, Y., Yi, W., Yang, J., Liu, J., Yi, D., Liang, H., Jin, Z., Reiter, R.J., Duan, W., Yu, S., 2017. Melatonin protects against the pathological cardiac hypertrophy induced by transverse aortic constriction through activating PGC-1beta–*in vivo* and *in vitro* studies. J. Pineal Res. 63 https://doi.org/10.1111/jpi.12433.